Available online at www.sciencedirect.com
ScienceDirect
Trans. Nonferrous Met. Soc. China 30(2020) 2311−2325
Transactions of Nonferrous Metals Society of China
www.tnmsc.cn

Relationship between amounts of low-melting-point eutectics and hot tearing susceptibility of ternary Al−Cu−Mg alloys during solidification

Jia-qiang HAN[1], Jun-sheng WANG[2,3], Ming-shan ZHANG[2,3], Kang-min NIU[1]

1. School of Materials Science and Engineering, University of Science and Technology Beijing, Beijing 100083, China;
2. School of Materials Science and Engineering, Beijing Institute of Technology, Beijing 100081, China;
3. Advanced Research Institute of Multidisciplinary Science, Beijing Institute of Technology, Beijing 100081, China

Received 28 December 2019; accepted 18 May 2020

Abstract: A systematical study on the relationship between the amounts of different eutectic phases especially the low-melting-point (LMP) eutectics and the hot tearing susceptibility of ternary Al−Cu−Mg alloys during solidification was performed. By controlling the concentrations of major alloying elements (Cu, Mg), the amounts of LMP eutectics at the final stages of solidification were varied and the corresponding hot tearing susceptibility (HTS) was determined. The results showed that the Al−4.6Cu−0.4Mg (wt.%) alloy, which contained the smallest fraction of LMP eutectics among the investigated alloys, was observed to be the most susceptible to hot tearing. With the amount of total residual liquid being approximately the same in the alloys, the hot tearing resistance is considered to be closely related to the amounts of LMP eutectics. Specifically, the higher the amount of LMP eutectics was, the lower the HTS of the alloy was. Further, the potential mechanism of low HTS for alloys with high amounts of LMP eutectics among ternary Al−Cu−Mg alloys was discussed in terms of feeding ability and permeability as well as total viscosity evolution during solidification.

Key words: Al−Cu−Mg alloy; hot tearing; solidification; eutectic reaction; low-melting-point (LMP) eutectics; thermodynamics

1 Introduction

Hot tearing has been one of the critical issues for mechanically casting and welding sound components. Many literatures [1−3] have reported that the occurrence of hot tearing in an alloy is mainly attributed to the volumetric shrinkage, thermal contraction and insufficient feeding at the final stage of solidification, during which the fraction of solid phase exceeds 80 vol.%. For multi-component Al alloys, many solutes will be rejected to the solid/liquid interface as solidification proceeds. Meanwhile, the binary, ternary or even quaternary eutectic reactions may successively take place once the solute levels exceed the corresponding critical values. Therefore, it is believed that the evolution of the residual liquid phase at intergranular channels will have a significant influence on the formation of hot tears [4,5].

The subject with respect to effects of intermetallic phase formation and eutectic reaction during solidification on the fluidity and feeding ability of residual liquid in ferrous and Al alloys has been reported several times. For instance, DASH and MAKHLOUF [6] reported that Fe and Si will be enriched in the residual liquid of Al−Si alloy, forming needle-like β-AlFeSi phases. These phases are located at interdendritic channels or grain boundaries, blocking liquid flow and hence promoting the formation of casting defects. Similarly, MOUSAVI et al [7] showed that high-melting-point Al−Fe eutectic phases block the interdendritic fluid flow and impede the feeding of shrinkage during the welding process of 7108 Al

Corresponding author: Jun-sheng WANG; Tel: +86-10-68915043; E-mail: junsheng.wang@bit.edu.cn
DOI: 10.1016/S1003-6326(20)65381-X

alloy. Recently, LIU and CHEN [8] have concluded that both the addition of Mn and combined additions of Mn and Zr into Al−Si−Cu 319 cast alloys can modify both the Fe-bearing intermetallics and the eutectic Si particles, improving the mechanical properties of the alloy in the semi-solid state. Moreover, the modification of the Fe-bearing intermetallics from platelet-like β-Fe to Chinese script α-Fe has been proven to be beneficial to the liquid flowing through dendritic channels and hence the hot tearing resistance.

In addition to intermetallics, many studies have demonstrated that the eutectic reaction in the residual liquid is another crucial factor influencing the fluidity of the liquid in mushy zones and hence hot tearing susceptibility (HTS). For example, MATSUDA et al [9] and LIPPOLD and SAVAGE [10] reported that the eutectic liquid, which is confined as liquid films distributing along grain boundaries or droplets located at triple junctions, makes the stainless steels more susceptible to hot cracking. This is supported by the results of AUCOTT et al [11] and it was indicated that the solute-rich, small liquid pockets can act as the initiator for cracking and hence promote the formation of hot cracking. However, the results reported by MATSUMOTO et al [12] confirmed that the healing of cracks by low-melting-point (LMP) eutectics will improve the solidification cracking resistance of boron-added 304 stainless steels. The inconsistent results regarding the effect of eutectic liquid on HTS obtained by MATSUDA et al [9], LIPPOLD and SAVAGE [10], AUCOTT et al [11] and MATSUMOTO et al [12] may be due to the indistinctness of different eutectic sequences and the combined effects of wetting and backfilling of eutectic liquid which solidifies at the last stage. Besides, CHIRKOV et al [13,14] investigated the fluidity variations of Al−Cu−Mg alloys as a function of major elements such as Cu and Mg, and minor elements such as V and Ti. It was pointed out that the LMP α-Al+θ+S eutectic liquids in Al−Cu−Mg alloys played a positive role in their fluidity. Nevertheless, they did not further discuss the corresponding HTS. LI et al [15] suggested that it was Zn-containing eutectics that promoted the formation of coalesced networks in Al−xZn−2Mg−2Cu (wt.%, unless stated otherwise) alloys. This results in a lower coherency solid fraction, which is a key parameter for many prediction models. TAGHIABADI et al [16] reported that Cu increases the HTS of A356 alloy and this is attributed to the addition of Cu widening the solidification range which in turn decreases its fluidity and increases the time exposed to the hot tearing susceptible zone. On balance, these studies have demonstrated the fact that the eutectic reactions in the residual liquid of alloys have a significant effect on the fluidity of liquid at mushy zones and hence the formation of various defects.

It is known to us that many hot tearing criteria have been established. According to the systematical evaluation of their validity by SUYITNO [17] and GHONCHEH et al [3], the Rappaz−Drezet−Gremaud (RDG) criterion from RAPPAZ et al [18] has the solid foundation in physics and can produce reasonable predictions in many cases. Based on this model, KOU [19] further derived a new model for hot cracking, which took into account the derivative of $|\mathrm{d}T/\mathrm{d}(f_s^{1/2})|$ near $(f_s)^{1/2}=1$. HAN et al [20] have systematically studied the hot cracking susceptibility of Al−Li alloys based on the KOU's model [19]. In general, to date, the driving forces for hot tearing have been well established but the theoretical models can only predict hot cracking in binary or simple alloy compositions. ESKIN and KATGERMAN [21] and CAMPBELL [4] pointed out that none of the existing criteria can give a quantitative prediction with respect to whether a hot tear will appear or not, and even its position, length, and shape. The reasons for the gaps between theoretical predictions and experimental results are mainly due to the complex nature of hot tearing and uncertainty of the crack initiation and propagation mechanism. Therefore, a more accurate description of the relationship between the solidification behavior of multi-component Al alloys and the corresponding HTS can help to improve our understanding and lead to development of hot tearing criteria for industrial alloys which are normally multi-component systems.

Since the eutectic reactions in residual liquids and the formation of hot tearing take place almost at the same stage, it is reasonable to believe that different eutectic reaction features have the unique effect on the HTS. To this end, in the present work, a series of Al−(5−x)Cu−xMg alloys have been prepared to rationalize the relationship between the amounts of different eutectics especially the LMP

eutectics and the corresponding HTS. The results obtained may help to further understand the hot tearing formation mechanism of multi- component Al alloys.

2 Experimental

In order to eliminate the effects of overall backfilling from residual liquid, the amounts of total residual liquid between the experimental alloys should be kept approximately the same. To this end, a series of alloys with constant Cu+Mg concentrations, Al−(5−*x*)Cu−*x*Mg (*x*=0, 0.4, 0.8, 1.2, 1.6 and 2.0) alloys were prepared using pure Al (99.9%), Al−50Cu and Al−50Mg master alloys. Pure Al was melted at 720 °C in a graphite crucible with a capacity of 1.5 kg using an electrical resistance furnace and the complete liquid metal was held above the melting temperature for 20 min. Then, the Al−Cu master alloy was added into the liquid metal and stirred for 1 min. After that, the procedure was repeated for the Al−Mg master alloy except that the temperature was reduced to 700 °C. Finally, the liquid alloy was directly poured into a pre-designed graphite mold. The composition of samples was measured by inductively coupled plasma atomic emission spectroscopy (ICP-AES, Thermo, MKII-M6) and listed in Table 1.

During the solidification of the samples in the pre-designed mold, the contraction load profiles versus time can be collected using the equipment shown in Fig. 1(a), which was developed by LI et al [22]. The setup was designed to simultaneously measure the contraction load, time as well as temperature with the T-shaped mold shown in Fig. 1(b). At the bottom of the mold, a hole was drilled to allow the insertion of a thermocouple. The measurement accuracy of the load cell was 0.05% in the entire load ranges and the data acquisition frequency was set to be 20 Hz. The detailed descriptions of the experimental setup and method to obtain the load values at non-

Table 1 Actual chemical composition of samples (wt.%)

Alloy	Cu	Mg	Fe	Si	Al
Al−5.0Cu	5.02	−	0.08	0.10	Bal.
Al−4.6Cu−0.4Mg	4.48	0.43	≤0.05	0.11	Bal.
Al−4.2Cu−0.8Mg	4.09	0.82	≤0.05	0.11	Bal.
Al−3.8Cu−1.2Mg	3.69	1.14	≤0.05	0.10	Bal.
Al−3.4Cu−1.6Mg	3.26	1.47	≤0.05	0.10	Bal.
Al−3.0Cu−2.0Mg	2.89	1.78	≤0.05	0.10	Bal.

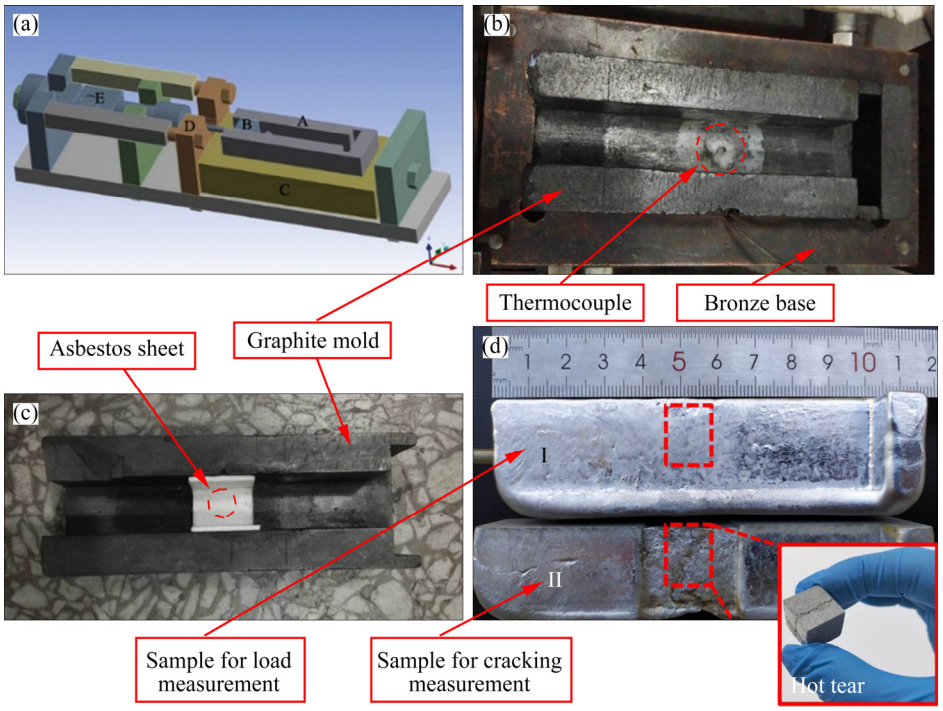

Fig. 1 (a) Experimental setup [15]; (b, c) Images of casting component inside cavity of mold where load and displacement were measured; (d) Typical T-shaped samples for load (I) and cracking (II) measurements (A—Graphite mold used for load and HTS measurement; B—Moving wall; C—Bronze base with special cooling channel; D—Fastener; E—Load cell)

equilibrium solidus (NES) and crack width for evaluating HTS can be found in previous publications [15,22−25]. The dimension of asbestos in this experiment was 20 mm × 20 mm × 20 mm, as shown in Fig. 1(c). Each set of experiment was repeated three times. The HTS evaluation in this experiment was based on the measurements of the maximum crack widths and contraction load values at NES. The NES points were calculated using the thermodynamic software JMatPro7.0 (Sente software Ltd., Guild, U.K.) based on the Scheil model and CALPHAD method.

Specimens for microstructure characterization were taken from locations close to thermocouples, which were indicated by the broken red rectangle lines for Sample I in Fig. 1(d). Every sample went through grounding, polishing, and finally etching in dilute Keller reagent for 10 s. In order to obtain the eutectic reaction details, differential scanning calorimetry (DSC, TA, SDT Q600) experiments were performed for every alloy. Porosity was statistically analyzed using Image J with noise removal for features less than 4 pixels. The microstructure analysis was performed using scanning electron microscope (SEM, ZEISS LEO1450), equipped with an energy dispersive spectroscopy (EDS, Thermo Scientific UltraDry).

3 Results

3.1 Solidification kinetics

DSC curves of the samples and the data extracted from the curves are shown in Fig. 2 and Table 2, respectively. The DSC curves in Fig. 2 showed two endothermic peaks, among which Peak I and Peak II corresponded to the eutectic reactions and the primary α(Al), respectively. Unfortunately, it should be noted that details of the eutectic reaction sequences could not be resolved in Peak I of the DSC curves in the present work. However, it can be qualitatively obtained that the fractions of total eutectic liquid in the samples were approximately kept the same by comparing the integrated area underneath the peaks relative to the total latent heat released from each specimen. The typically measured cooling curves during solidification of the samples are shown in Fig. 3(a). The two plateaus of the curves correspond to the phase transformation of α(Al) and eutectic. From Fig. 3(a), the transformation temperature ranges for α(Al) and eutectic reactions showed consistent with the DSC results in Fig. 2 and Table 2. Because both the DSC results and cooling curves could not differentiate the binary, ternary, quaternary eutectic

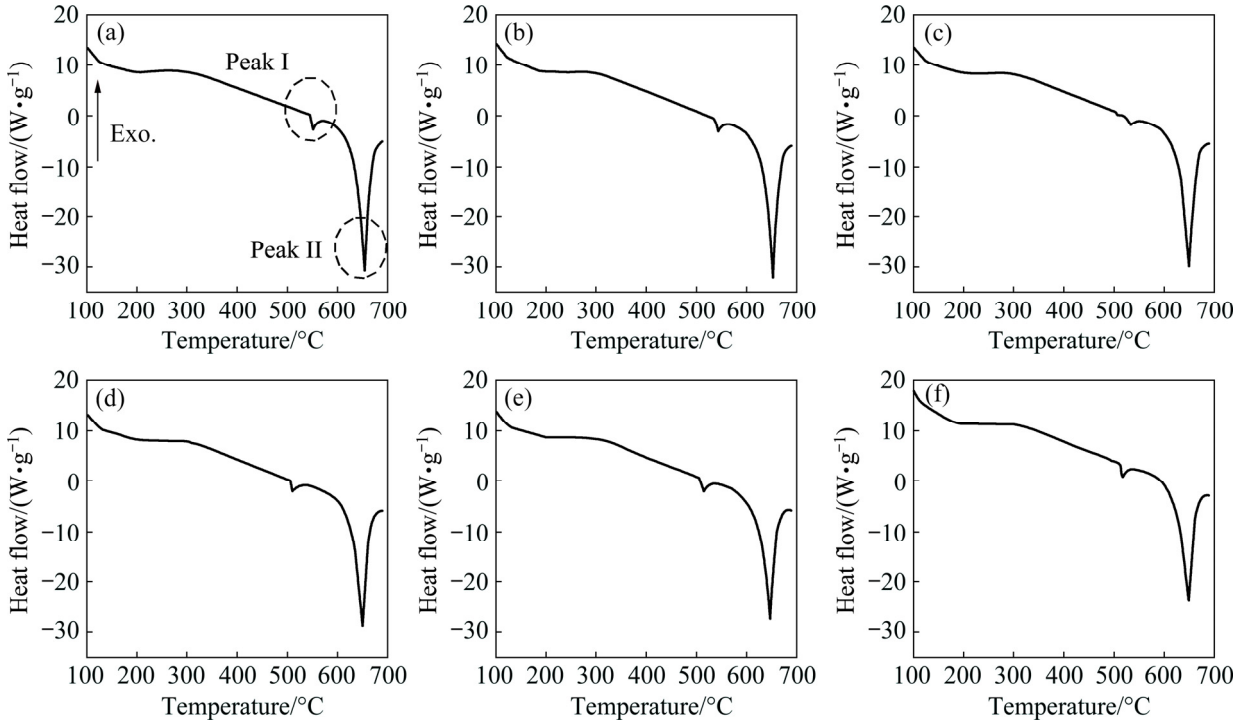

Fig. 2 DSC curves of Al−(5−x)Cu−xMg alloys: (a) x=0; (b) x=0.4; (c) x=0.8; (d) x=1.2; (e) x=1.6; (f) x=2.0

Table 2 Temperature and enthalpy extracted from DSC curves of samples

Alloy	Peak I (eutectic)			Peak II (α(Al))		
	Onset temperature/°C	Peak temperature/°C	Enthalpy/ (J·g^{-1})	Onset temperature/°C	Peak temperature/°C	Enthalpy/ (J·g^{-1})
Al−5.0Cu	547.46	550.62	10.21	636.08	653.71	250.3
Al−4.6Cu−0.4Mg	536.83	542.70	9.67	634.83	652.03	270.8
Al−4.2Cu−0.8Mg	524.91	533.68	6.04	632.35	650.40	278.1
Al−3.8Cu−1.2Mg	506.39	509.51	9.49	629.21	649.27	264.1
Al−3.4Cu−1.6Mg	508.72	514.84	13.15	627.58	646.66	282.0
Al−3.0Cu−2.0Mg	513.44	517.48	10.25	626.45	648.98	249.7

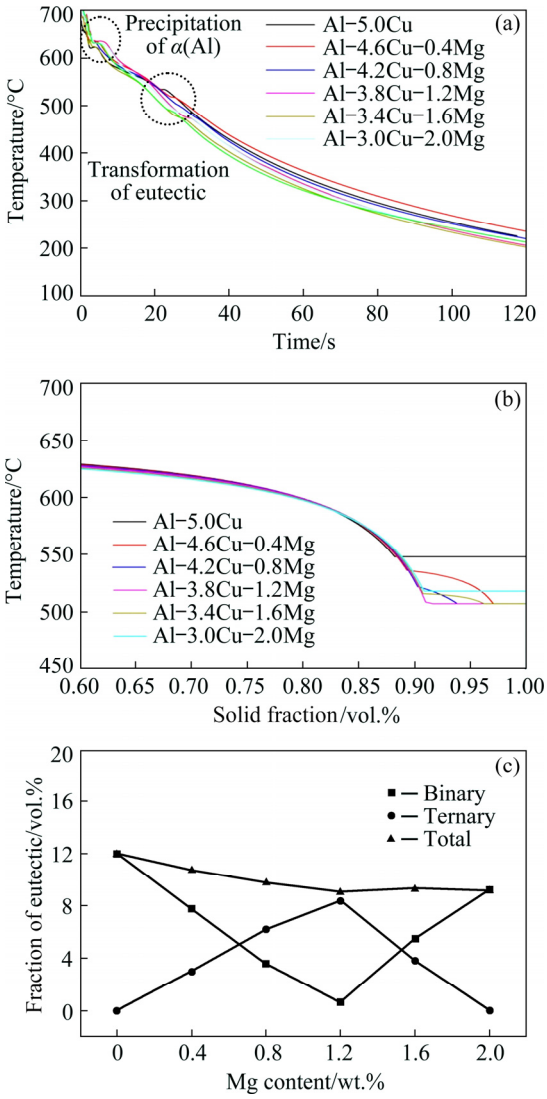

Fig. 3 Cooling curves of alloy tested in this study (a), calculated temperature as function of solid fraction (b) and predicted volume fraction of binary, ternary, and total eutectics as function of Mg content (c)

reactions in the residual liquid, the eutectic reaction sequences at different temperatures and solid fractions, and NES points were calculated using a thermodynamic software JMatPro 7.0 as shown in Figs. 3(b, c) and listed in Table 3.

Table 3 Eutectic reaction sequences from Scheil calculation

Alloy	Eutectic precipitation sequence	NES point/°C
Al−5.0Cu	$L\rightarrow\alpha$(Al)+Al_2Cu	548
Al−4.6Cu−0.4Mg	$L\rightarrow\alpha$(Al)+Al_2Cu $L\rightarrow\alpha$(Al)+Al_2Cu+Al_2CuMg	507
Al−4.2Cu−0.8Mg	$L\rightarrow\alpha$(Al)+Al_2Cu $L\rightarrow\alpha$(Al)+Al_2Cu+Al_2CuMg	507
Al−3.8Cu−1.2Mg	$L\rightarrow\alpha$(Al)+Al_2CuMg $L\rightarrow\alpha$(Al)+Al_2Cu+Al_2CuMg	507
Al−3.4Cu−1.6Mg	$L\rightarrow\alpha$(Al)+Al_2CuMg $L\rightarrow\alpha$(Al)+Al_2Cu+Al_2CuMg	507
Al−3.0Cu−2.0Mg	$L\rightarrow\alpha$(Al)+Al_2CuMg	518

As shown in Fig. 3(b) and Table 3, a common feature of the profiles was that there were two typical eutectic transformations after primary α(Al) precipitated in the ternary Al−Cu−Mg alloys. First, the monovariant eutectic reaction, $L\rightarrow\alpha$(Al)+Al_2Cu, occurred. Then, if some liquid still remained after the monovariant reaction, the solidification process was usually completed with an invariant eutectic reaction $L\rightarrow\alpha$(Al)+Al_2Cu+Al_2CuMg, which was named LMP eutectics. The total residual liquid fraction after the completed precipitation of primary α(Al), the monovariant and the invariant eutectic fractions can also be extracted from the T versus f_s profiles based on the thermodynamic database, which was shown in Fig. 3(c). It can be seen from Fig. 3(c) that the amounts of different eutectic reaction sequences in the alloys showed continuous variations while the total amounts of the residual

eutectic liquids after the precipitation of primary α(Al) approximately remained the same except slight decrease as the Mg content increased. The NES points calculated are also shown in Table 3. It was found that for the alloys containing 0.8% Mg or more, the calculated NES temperatures were consistent with the onset temperature of Peak I in the DSC experiments; however, for the alloy with 0.4% Mg, the inconsistency may result from the relative low amount of the Al_2CuMg LMP eutectics, which could not be detected in the DSC experiments.

3.2 Crack width

It has been reported that the widths of the main cracks on test samples can be used as an index to qualitatively evaluate the HTS of an alloy [15,23]. Figure 4 shows the macroscopic images of typical main cracks on the surface of test samples taken by stereomicroscope. The crack widths were measured by Image J. The maximum crack width along the length direction as a function of Mg content is shown in Fig. 5(a). Variations of Mg content could give rise to different amounts of eutectic in the residual liquid of the alloys. As can be seen in Fig. 5(a), the maximum crack width first decreased from 1.18 mm for the Al−5Cu alloy to 0.67 mm for the Al−4.6Cu−0.4Mg alloy, and finally reached 0.76 mm for the Al−3.0Cu−2.0Mg alloy after some fluctuations. It is of great importance to notice in Fig. 5(a) that the crack width does not exhibit a linear relationship as the Mg content changes.

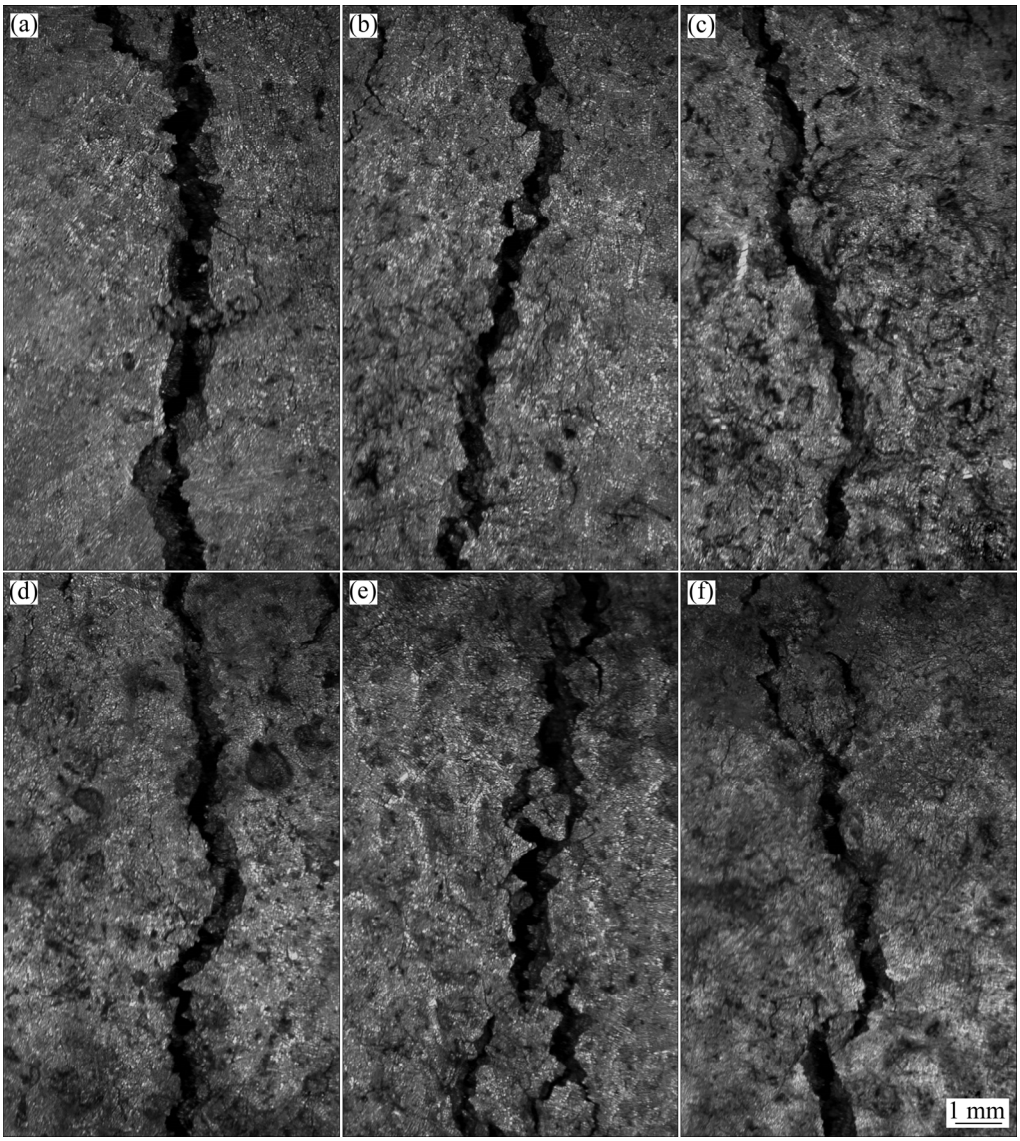

Fig. 4 Macroscopic images of hot tears on external surface of Al−(5−x)Cu−xMg alloys: (a) x=0; (b) x=0.4; (c) x=0.8; (d) x=1.2; (e) x=1.6; (f) x=2.0

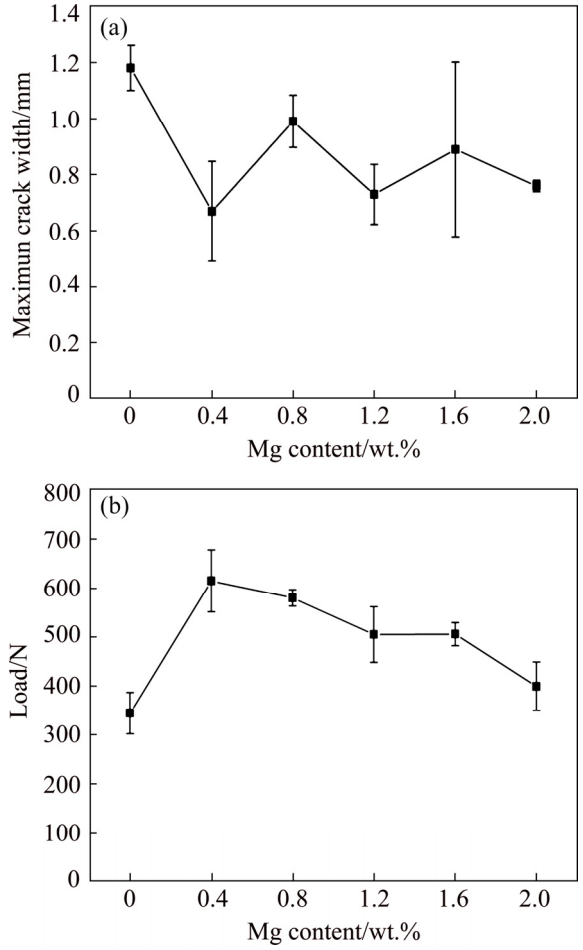

Fig. 5 Maximum widths of cracks on samples (a) and load values at NES as function of Mg content (b)

3.3 Load development

As has been reported by CAMPBELL [4], hot tearing is mainly attributed to the uniaxial tensile failure in a weak material. Therefore, the evolution of contraction stress during solidification especially at the final stage is a critical factor for the formation of hot tears. LI et al [22], EASTON et al [23] and SABAU et al [24] have adopted the load evolution to evaluate the HTS of alloys. As demonstrated to be a good HTS index for Al alloys by LI et al [22] and EASTON et al [23], the load values at NES were obtained based on the thermodynamic calculations, cooling curves and load. The detailed process can be found in the works reported by LI et al [22] and is shown in Fig. 6. The load values at NES as a function of Mg content are shown in Fig. 5(b). The load values at NES first rapidly increased to the maximum and then gradually decreased as the Mg content varied. Using the evaluation method employed by LI et al [22] and EASTON et al [23], the Al−4.6Cu−0.4Mg alloy showed the maximum load values at NES. This indicated that this alloy was the most sensitive to hot tearing among the alloys in this study.

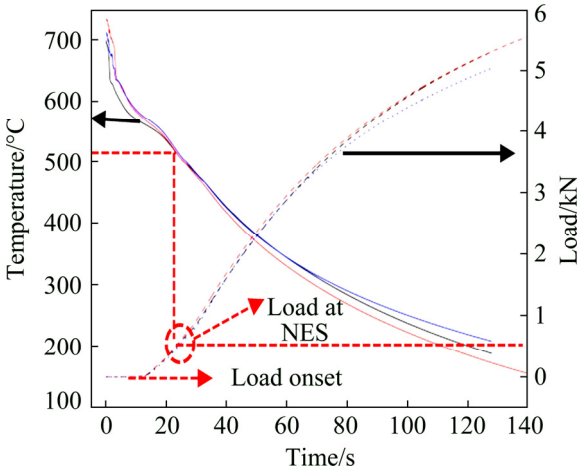

Fig. 6 Cooling curves (solid line) and load curves (dash line) of Al−4.2Cu−0.8Mg alloy measured during solidification process combined with NES from thermodynamic calculations to obtain load values at NES

3.4 Microstructure analysis

Microstructures of the samples located next to thermocouples are shown in Fig. 7. It can be observed in Fig. 7 that except for the alloy with 0.4% Mg, other alloys all showed significant amounts of LMP eutectics (as indicated by the broken red arrows). The alloy with 0.4% Mg displayed only monovariant eutectic features (as indicated by the broken blue arrows) with negligible amounts of LMP eutectics. Moreover, it can also be seen from Fig. 7 that while the alloys with 0.8%, 1.2% and 1.6% Mg showed two types of eutectics, the alloy with 2.0% Mg showed only the typical LMP eutectics. This is in good correlation with the solidification sequences predicted by thermodynamic software, as shown in Table 3. The alloy with 0.4% Mg did not show the two types of eutectic and only one type of eutectic feature may be attributed to the extremely low amount of LMP eutectics. This unique microstructure feature for the alloy with 0.4% Mg will inevitably make the backfilling and interdendritic bridging at the final solidification stage significantly different from other alloys. The fracture morphologies of hot tears are shown in Fig. 8 and appear to have typical dendritic morphologies and brittle fracture features.

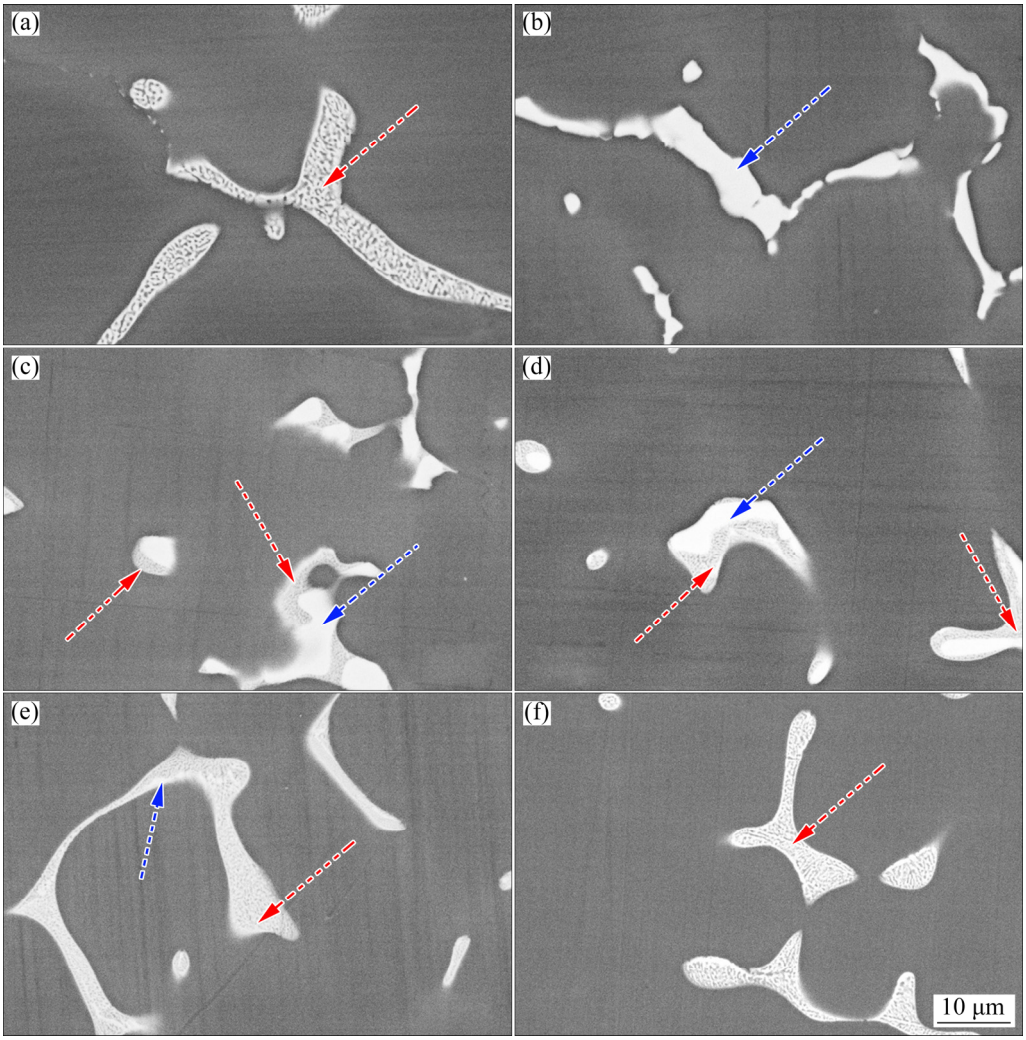

Fig. 7 Microstructure of Al−(5−*x*)Cu−*x*Mg alloys: (a) *x*=0; (b) *x*=0.4; (c) *x*=0.8; (d) *x*=1.2; (e) *x*=1.6; (f) *x*=2.0

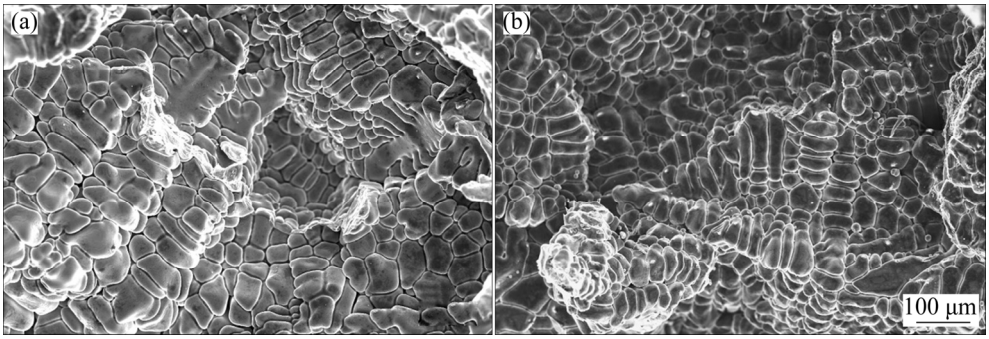

Fig. 8 Fracture morphologies of hot tear surfaces: (a) Al−5Cu; (b) Al−4.6Cu−0.4Mg

4 Discussion

One of the critical steps in this study is keeping the total amounts of the residual liquid the same and only varying the eutectic reaction sequence. This is attributed to the fact that the amount of total residual liquid has a significant influence on the healing of hot cracks. It is worth mentioning that when the solidified structures between Al alloys are similar, the amount of residual liquid of alloys is proportional to the point at which dendrites begin to cohere with each other and transmit load [22]. Therefore, the load onset temperatures and the corresponding solid fractions during solidification of the investigated alloys are

shown in Fig. 9. The results were obtained by combining the cooling curves and thermodynamic calculations, as shown in Fig. 6 and Fig. 3(b). As can be seen from Fig. 9, the load onset temperatures and the corresponding solid fractions were similar among the six alloys. Therefore, it can be concluded that the total amounts of residual eutectic liquid were approximately the same among the six alloys. In addition, the DSC curves in Fig. 2 and thermodynamic calculations in Figs. 3(b, c) also supported this pre-requirement.

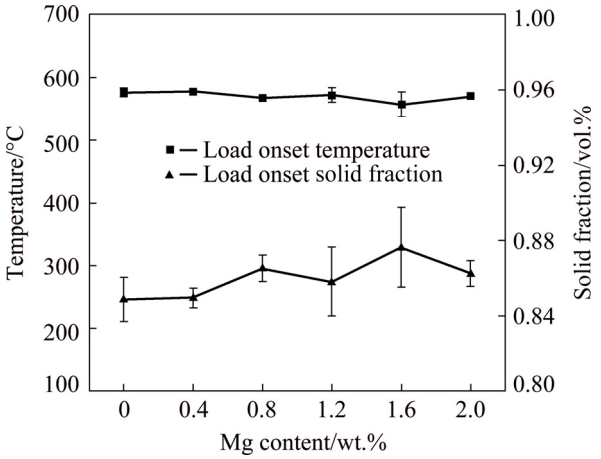

Fig. 9 Onset temperature and corresponding solid fraction

It should be noted that a good correlation between the measured crack width and load at NES as a function of Mg content was not achieved in the present work, as shown in Fig. 5. This is inconsistent with the results obtained by EASTON et al [23] and LI et al [15]. SPITTLE and CUSHWAY [26] pointed out that there exist a number of fundamental questions in relating the size of cracks on the external surface of castings to its HTS. At the same time, they also listed some questions, i.e., whether the susceptibility is really proportional to the crack size and why should an alloy exhibiting only one crack that fractured completely be defined as less susceptible than the one that cracks in many places and exhibits a greater crack length.

In an attempt to explain the relationship between crack width and hot tearing susceptibility referred to in the present work, a micromechanical model is proposed. As shown in Fig. 10, the formation of hot tearing can be roughly divided into three stages: (1) Some pores and oxide inclusions

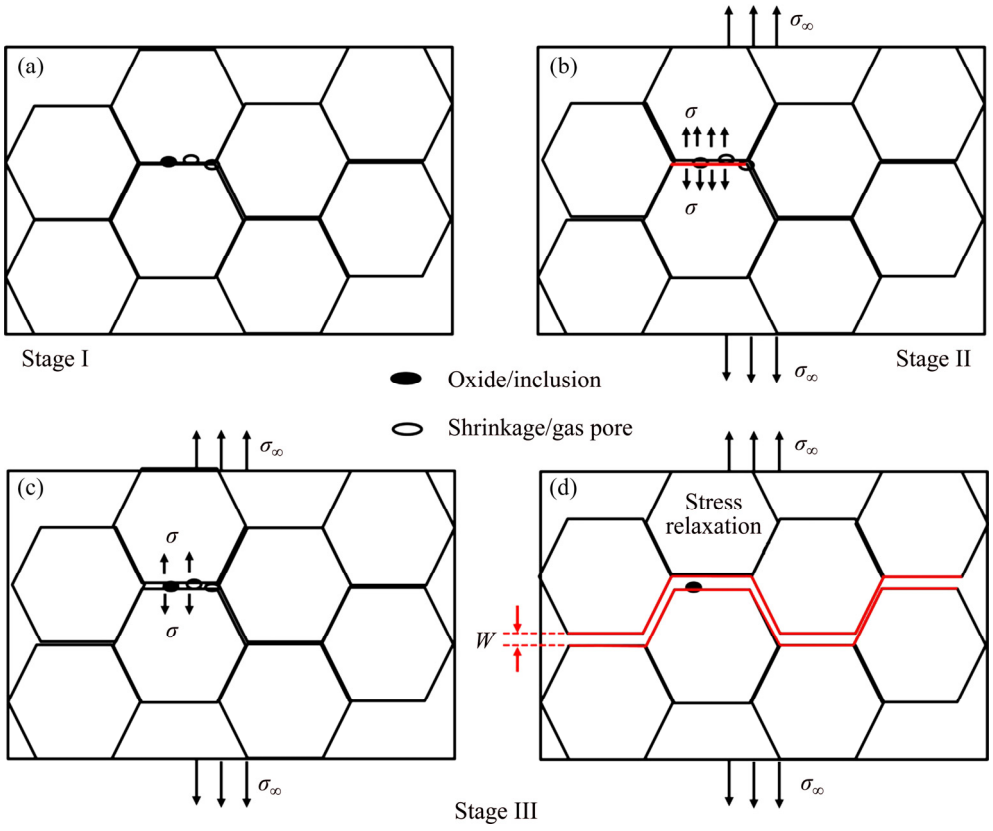

Fig. 10 Schematic of micromechanical model of hot tearing: (a) Stage I, defects accumulation; (b) Stage II, stress concentration; (c, d) Stage III, crack propagation and stress relaxation (σ_∞ and σ represent remote and local stress, respectively)

accumulate at grain boundaries, as shown in Fig. 10(a); (2) Stress concentration upon pores or oxides starts occurring at grain boundaries due to shrinkage and thermal contraction. According to the GRIFFITH's model [27], defects that have small curvature radii can be equivalent to micro-cracks. When the stress concentration reaches a critical level, the equivalent micro-cracks will become unstable, as shown in Fig. 10(b); (3) As the stress concentration level further increases, the crack will propagate along the grain boundaries that are covered by liquid films and brittle fracture will occur, as shown in Figs. 10(c, d).

The hot tear formation process is accompanied by the release of stress and the creation of new surfaces. According to the Griffith's fracture model [27], the energy change caused by stress release is conserved with the surface energy of the new surface formed. In addition, the crack propagation may also be the coalescence of several micro-cracks. Therefore, either from the perspective of energy or the propagation of cracks, the crack width on the sample surface cannot be a good indicator for HTS. Therefore, our results support the previous comments on reliability of using crack size on the surface of castings for evaluating of crack susceptibilities [26]. Finally, it is worth mentioning that the crack width on the sample surface is different from the crack tip opening displacement (CTOD) proposed by WELLS [28] for the fracture of ideal elastic−plastic materials.

However, according to CAMPBELL [4], uniaxial tensile is the major driving force for the formation of hot tearing. Besides, EASTON et al [23,29], LI et al [15], SABAU et al [24] and SWEET et al [30] have studied the HTS by measuring the evolution of contraction stress during solidification and the conclusion has been made that it is rational to believe that the greater the stress accumulation at NES, the greater susceptibility of an alloy to cracking will be. In this work, the alloy containing 0.4% Mg showed the largest load value at NES (Fig. 5(b)) and thus was considered to have the highest HTS among the six alloys. Since different alloys have different eutectic reaction sequences (Table 3), it can be further concluded that it is the difference in eutectic reactions and its volume fraction that result in the significantly different susceptibilities of hot tearing in the six alloys. Specifically, that is, the lower the amount of the LMP eutectics, the greater the sensitivity to cracking of an alloy.

To further validate the relationship between LMP eutectics and HTS proposed above, the load at NES as a function of the amounts of LMP eutectics in the six alloys is shown in Fig. 11. It can be seen that as the amount of LMP eutectics increased, the values of load at NES decreased. Combining the results in the present work and previous publications [4,15,23], it can be further concluded that the amount of LMP eutectics can be regarded as another HTS index for multi-component Al alloys with similar amounts of residual liquid.

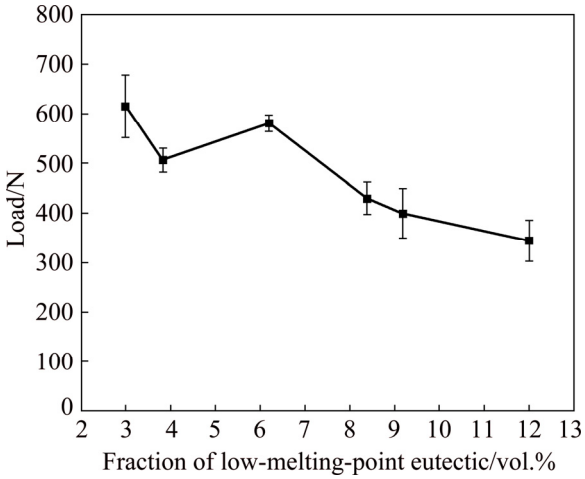

Fig. 11 Load values at NES as function of amount of LMP eutectics

HTS has been reported to be extensively influenced by the backfilling of residual liquid [4,31] and shrinkage/gas pores possibly play an important role in the formation of hot tears if the backfilling at the final stage was impeded [4,32]. The distribution of the equivalent radius of pores is shown in Fig. 12. Among the six alloys, the distribution features were similar; however, some differences in the distribution of pores larger than 5 μm were shown in the insets. Different from other alloys, the Al−4.6Cu−0.4Mg showed some relatively large pores, of which the equivalent radius could reach 30−36 μm. These large pores showed the potential to promote the nucleation and propagation of hot tears. As seen in Table 3, the major eutectic reaction of the Al−4.6Cu−0.4Mg alloy was $L\rightarrow\alpha(\mathrm{Al})+\mathrm{Al_2Cu}$ monovariant transformation followed by a small amount of $L\rightarrow\alpha(\mathrm{Al})+\mathrm{Al_2Cu}+\mathrm{Al_2CuMg}$ low-melting-point/ invariant transformation.

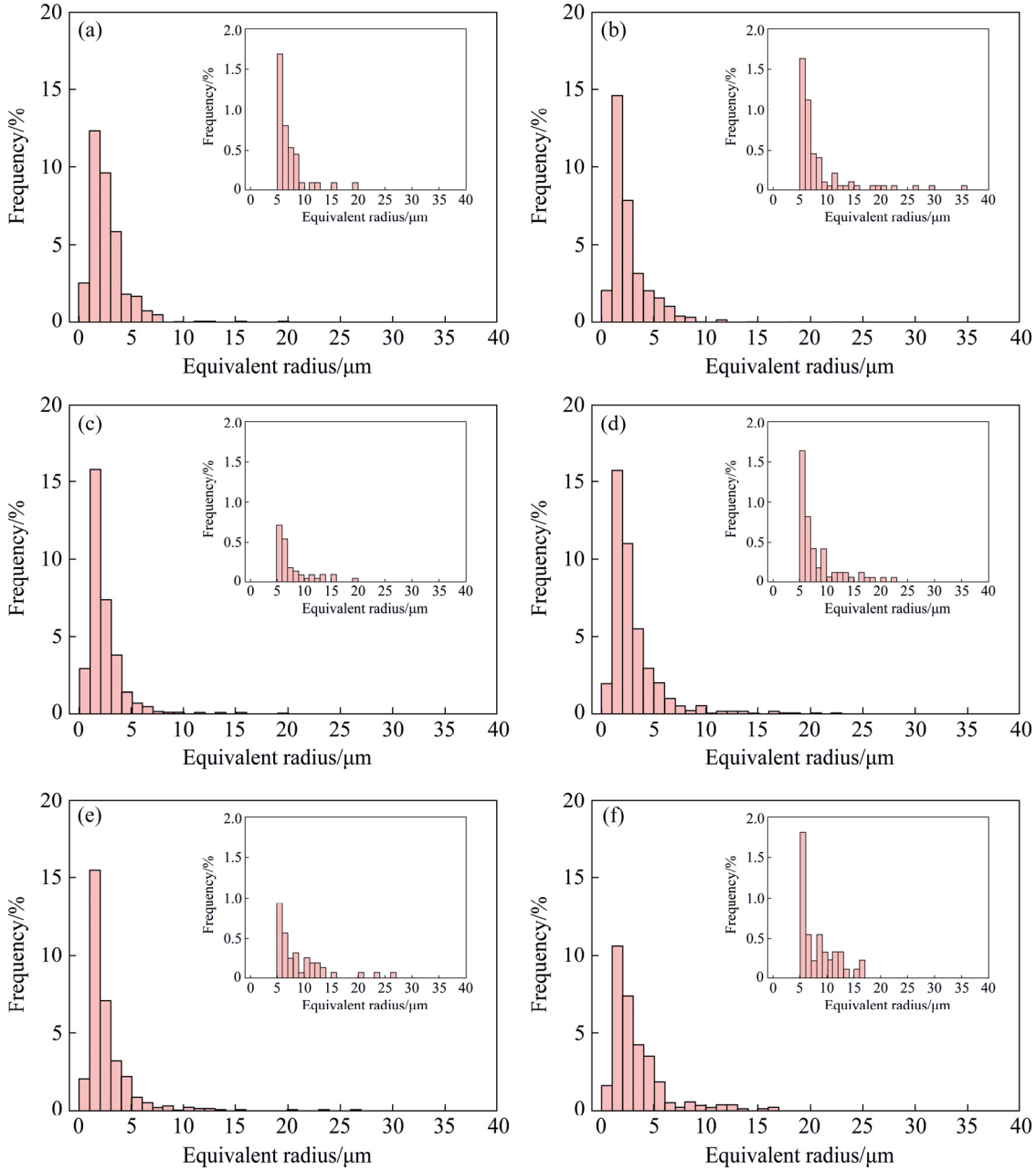

Fig. 12 Distribution of equivalent radius of pores in Al−(5−*x*)Cu−*x*Mg alloys: (a) *x*=0; (b) *x*=0.4; (c) *x*=0.8; (d) *x*=1.2; (e) *x*=1.6; (f) *x*=2.0

Based on the thermodynamic calculations, the volume fractions of total residual eutectic liquid, monovariant and invariant eutectic in the Al−4.6Cu−0.4Mg alloy were 10.719%, 7.731%, and 2.988%, respectively. It is worth noting that when the $L\rightarrow\alpha(Al)+Al_2Cu$ monovariant transformation completes, the solidification process will enter the vulnerable stage for hot tearing. At this time, the amount of $L\rightarrow\alpha(Al)+Al_2Cu+Al_2CuMg$ LMP eutectics determines the healing for cracks that have already formed due to the shrinkage of both α(Al) and monovariant eutectic transformations. However, if the amount of LMP eutectics of an alloy was relatively low such as the alloy with 0.4% Mg, the pore with large size would form, resulting from lack of backfilling for the shrinkage of α(Al) and Al_2Cu transformations.

The difference in the size distribution of pores can also be explained by the permeability evolution of alloys during solidification. The permeability values (K) of the alloys were calculated through a one-dimensional simple Kozeny−Carman analytical equation, $K=\lambda_2^3(1-f_s)^3/(180f_s^2)$ [33], in which, secondary dendrite arm spacing (SDAS, λ_2) and

solid fraction (f_s) were obtained from the thermodynamic calculations. Figure 13(a) shows the permeability variations as a function of temperature during solidification. Figure 13(b) shows the permeability values at NES as a function of the volume fraction of LMP eutectics. From Fig. 13, it can be observed that the Al−4.6Cu−0.4Mg alloy has relatively low permeability at the final stage of solidification and the permeability values of the alloy at NES increased remarkably as the amount of LMP eutectics increased. The low permeability will result in insufficient backfilling and promote the formation of pores.

Figure 14 shows the fracture morphologies of two typical samples: Al−5Cu and Al−4.6Cu−0.4Mg. It can be seen from the SEM images and EDS results in Fig. 14 that the eutectic phase of Al−5Cu alloy is mainly the α(Al)+Al_2Cu invariant eutectics phase. With the addition of 0.4% Mg, the eutectic reaction sequence changed from total

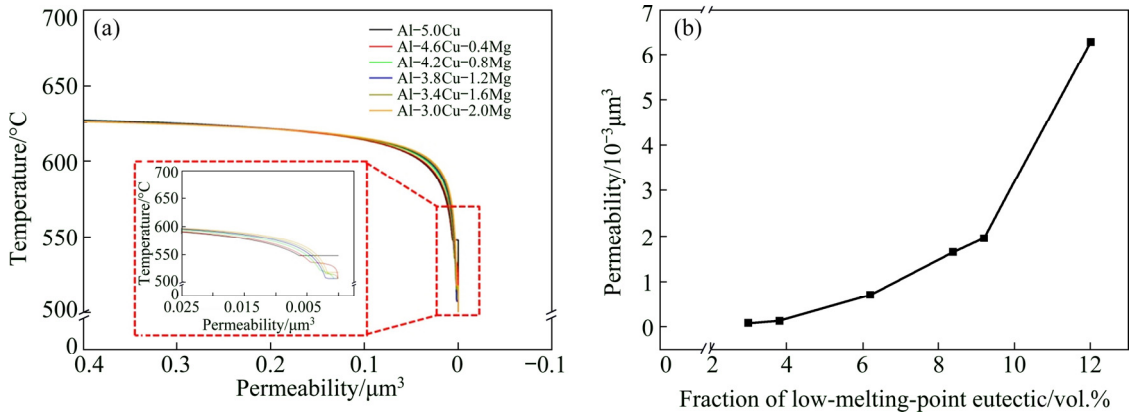

Fig. 13 One dimensional permeability results of investigated alloys based on Kozeny−Carman relation [33]: (a) Variations of permeability with temperature; (b) Permeability at NES as function of fraction of LMP eutectics

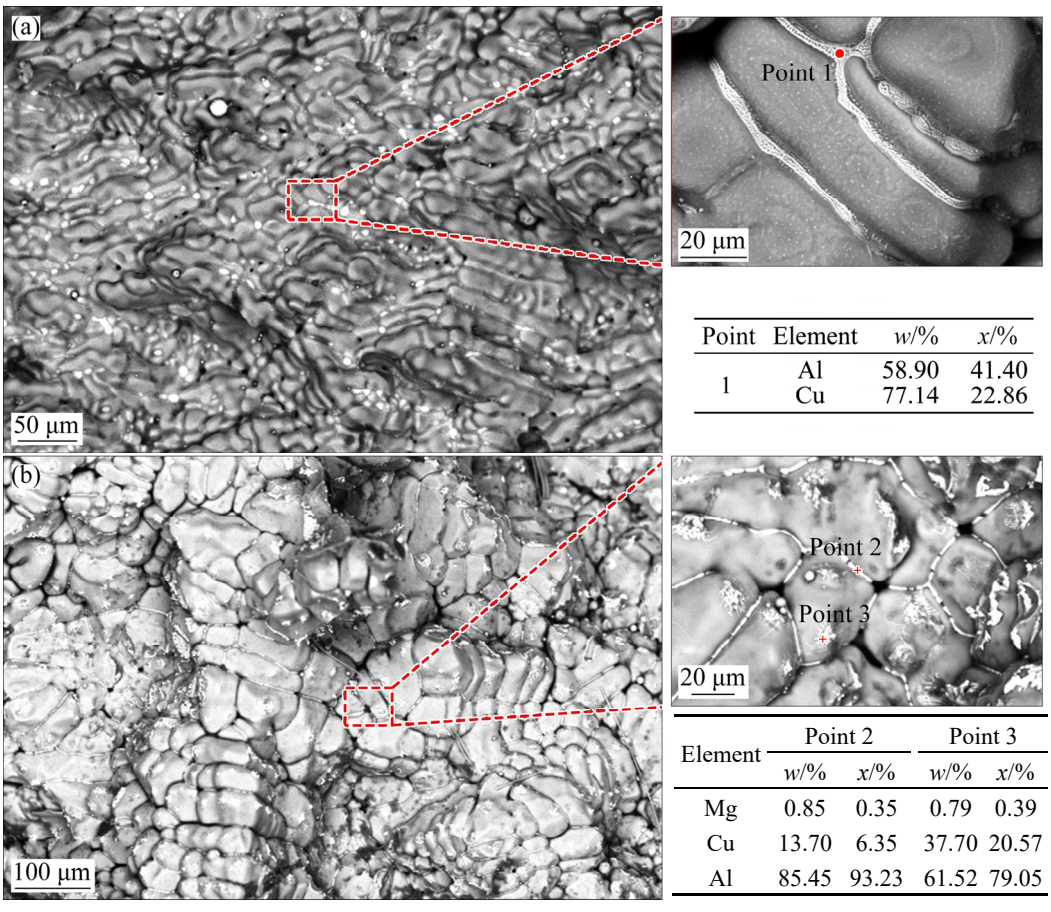

Point	Element	*w*/%	*x*/%
1	Al	58.90	41.40
	Cu	77.14	22.86

Element	Point 2		Point 3	
	w/%	*x*/%	*w*/%	*x*/%
Mg	0.85	0.35	0.79	0.39
Cu	13.70	6.35	37.70	20.57
Al	85.45	93.23	61.52	79.05

Fig. 14 Fracture morphologies and EDS results of hot tear surface: (a) Al−5Cu; (b) Al−4.6Cu−0.4Mg

$L\rightarrow\alpha(Al)+Al_2Cu$ to $L\rightarrow\alpha(Al)+Al_2Cu$ followed by $L\rightarrow\alpha(Al)+Al_2Cu+Al_2CuMg$. In the Al−4.6Cu−0.4Mg alloy, the monovariant $\alpha(Al)+Al_2Cu$ eutectic phase mainly nucleates at the primary $\alpha(Al)$ dendrites or grain boundaries and grows. This may hinder the backfilling of the residual liquid. Unlike the Al−Cu alloy where the solidification completes with abundant $\alpha(Al)+Al_2Cu$ invariant eutectics which can provide sufficient feeding to the shrinkage of $\alpha(Al)$, in the Al−4.6Cu−0.4Mg alloy the solidification completes with $\alpha(Al)+Al_2Cu+Al_2CuMg$ invariant eutectic reaction and the shrinkage of monovariant $\alpha(Al)+Al_2Cu$ eutectic reaction cannot be sufficient feeding due to the low amount of the invariant eutectic liquid. Therefore, many pores are expected to form between grains and dendrites in the Al−4.6Cu−0.4Mg alloy due to both the low amount of the invariant eutectic liquid and the blocking of feeding channels, as shown in Fig. 14(b). However, in the Al−5Cu alloy, the interdendritic channels are full of LMP eutectics liquid due to its large amount and hence relatively insensitive to hot tearing, as shown in Fig. 14(a). These results show good agreement with the findings by EASTON et al [23] that the monovariant eutectic is observed to have a negative role in the hot tearing resistance while the invariant eutectic reactions have a positive effect in multi-component Al alloys.

Besides, many researchers have pointed out that the formation of hot tears also closely relates to the mechanical behavior or rheological property of alloys in the semi-solid state [2,34]. The mechanical response of an alloy in the semi-solid state depends on its total viscosity at a temperature above the solidus. Figure 15 shows the calculated total viscosity evolution of the investigated alloys during solidification process and the values at NES as a function of the amounts of LMP eutectics. As can be seen in Fig. 15, the total viscosity of Al−4.6Cu−0.4Mg alloy was larger than other alloys at the final stage of solidification. In addition, the total viscosity at NES of the experimental alloys decreased remarkably as the amount of LMP eutectics increased in Fig. 15(b). This is consistent with the results demonstrated by permeability. It can be inferred from Fig. 15 that the monovariant eutectic phase attaching to the primary $\alpha(Al)$ promoted bridging between dendrites and grains, transmitting contraction stress through the network

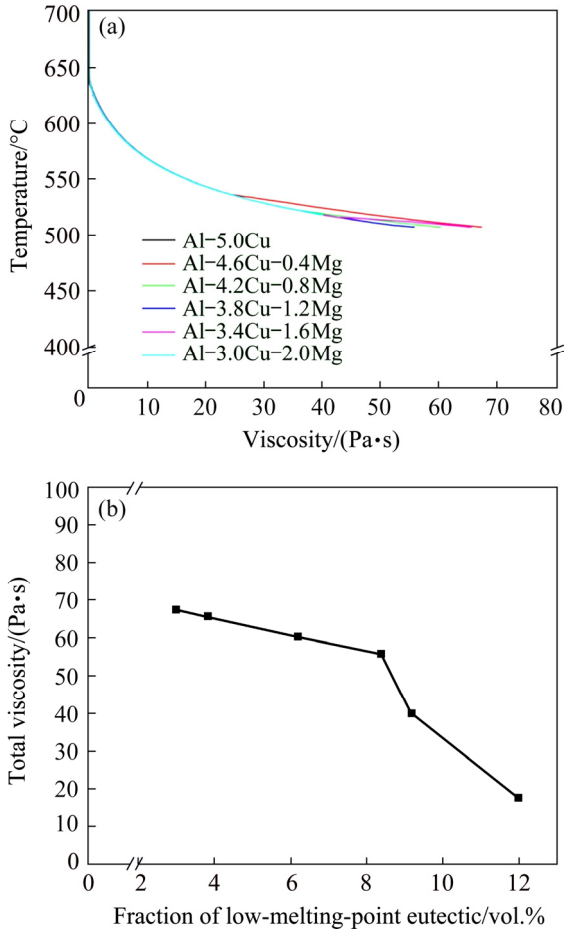

Fig. 15 Total viscosity evolution of six alloys during solidification process (a) and corresponding values at NES as function of amounts of LMP eutectics (b)

and hence contributing to the rheological resistance. The evidence of bridging between grains is shown in Fig. 16 by the broken red circles. It can be obtained from the EDS results in Table 4 that the intergranular bridging of Al−4.6Cu−0.4Mg may be $\alpha(Al)+Al_2Cu$ eutectic phase. It is worth noting that the force being transmitted through the dendrite network is one of the necessary factors for hot

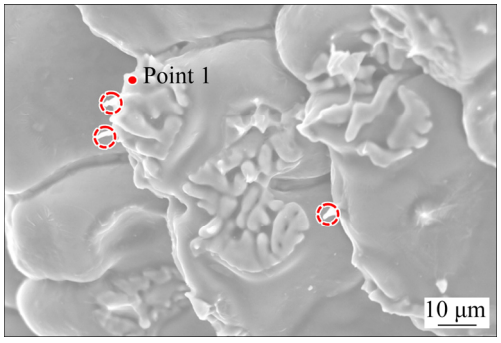

Fig. 16 Experimental evidence of bridging between grains and/or dendrites

Table 4 EDS results of phase shown by Point 1 in Fig. 16

Element	*w*/%	*x*/%
O	21.43	32.86
Mg	0.52	0.52
Cu	8.29	3.2
Al	69.76	63.42

tearing formation. Finally, the presence of the oxygen element further manifested the typical feature of the hot tear surface that the cracks could form at high temperatures and severe oxidation could be worsening the problem.

5 Conclusions

(1) The eutectic reactions at the final stage of solidification showed a significant effect on the HTS of Al−Cu−Mg alloys. The monovariant eutectics played a negative role in the resistance of hot tear formation while the LMP eutectics showed the opposite.

(2) Reduction in the volume fraction of LMP eutectics resulted in insufficient backfilling for the shrinkage of the monovariant eutectic solidification, which could also impede the backfilling of LMP eutectics. Moreover, the monovariant eutectics could promote bridging between grains or dendrites, making the Al−4.6Cu−0.4Mg alloy most sensitive to hot tearing among the alloys investigated.

(3) When the healing ability of residual liquid is considered in the study of HTS for multi-component Al alloys, it is not suitable to treat the residual liquid as a stable phase and the eutectic reactions in the residual liquid should be considered. It is the LMP eutectics that show relatively good backfilling ability and hence beneficial to the hot tearing resistance.

Acknowledgements

The authors would like to thank all labmates in the Integrated Computational Materials Engineering lab, Advanced Research Institute of Multidisciplinary Science, Beijing Institute of Technology. Many thanks to Hong-xiang LI, associate professor and Zhao-rui ZHANG, a PhD candidate in the State Key Laboratory for Advanced Metals and Materials, University of Science and Technology Beijing for their help with the training on the experimental equipment.

References

[1] BICHLER L, ELSAYED A, LEE L, RAVINDRAN C. Influence of mold and pouring temperatures on hot tearing susceptibility of AZ91d magnesium alloy [J]. International Journal of Metalcasting, 2008, 2: 43−54.

[2] ESKIN D G, SUYITNO, KATGERMAN L. Mechanical properties in the semi-solid state and hot tearing of aluminum alloys [J]. Progress in Materials Science, 2004, 49: 629−711.

[3] GHONCHEH M H, SHABESTARI S G, ASGARI A, KARIMZADEH M. Nonmechanical criteria proposed for prediction of hot tearing sensitivity in 2024 aluminum alloy [J]. Transactions of Nonferrous Metals Society of China, 2018, 28: 848−857.

[4] CAMPBELL J. Castings [M]. 2nd ed. Oxford: Elsevier, 2003.

[5] HOLT M, OLSON D L, CROESS C E. Interfacial tension driven fluid flow model for hot cracking [J]. Scripta Metallurgica et Materialia, 1992, 26: 1119−1124.

[6] DASH M, MAKHLOUF M. Effect of key alloying elements on the feeding characteristics of aluminum–silicon casting alloys [J]. Journal of Light Metals, 2002, 2: 251−265.

[7] MOUSAVI M G, CROSS C E, GRONG O. The effect of high-temperature eutectic-forming impurities on aluminum 7108 weldability [J]. Welding Journal, 2009, 88: 104−110.

[8] LIU K, CHEN X G. Influence of the modification of iron-bearing intermetallic and eutectic Si on the mechanical behavior near the solidus temperature in Al−Si−Cu 319 cast alloy [J]. Physica B: Condensed Matter, 2019, 560: 126−132.

[9] MATSUDA F, NAKAGAWA H, UEHARA T, KATAYAMA S, ARATA Y. A new explanation for role of delta-ferrite improving weld solidification crack susceptibility in austenitic stainless steel [J]. Transaction of JWRI, 1979, 8: 105−112.

[10] LIPPOLD J C, SAVAGE W F. Solidification of austenitic stainless steel weldments: Part III. The effect of solidification behavior on hot cracking susceptibility [J]. Welding Journal, 1982, 12: 388s−396s.

[11] AUCOTT L, HUANG D, DONG H B, WEN, S W, MARSDEN J, RACK A, COCKS A C F. A three-stage mechanistic model for solidification cracking during welding of steel [J]. Metallurgical and Materials Transactions A, 2018, 49: 1674−1682.

[12] MATSUMOTO T, SHINODA T, MIYAKE H, MATSUZAKA T, KANAI H. Effect of low-melting-point eutectic on solidification cracking susceptibility of boron-added AlSi 304 stainless steel welds [J]. Welding Journal, 1995, 74(12): 397−405.

[13] CHIRKOV E F. Laws of fluidity variation for aluminium alloys of Al−Cu−Mg-system [J]. Materials Science Forum, 1996, 217−222: 265−270.

[14] CHIRKOV E F, DOLZHANSKI Y M, FRIDLYANDER I N. Change of fluidity of aluminum superalloy 1151 (Al−Cu−Mg) during its alloying by transition metals [J]. Materials Science Forum, 2000, 331−337: 331−336.

[15] LI Y, GAO X, ZHANG Z R, XIAO W L, LI H X, DU Q, KATGERMAN L, ZHANG J S, ZHUANG L Z.

Experimental and theoretical studies of the hot tearing behavior of Al−*x*Zn−2Mg−2Cu alloys [J]. Metallurgical and Materials Transactions A, 2017, 48: 4744−4754.

[16] TAGHIABADI R, FAYEGH A, PAKBIN A, NAZARI M, GHONCHEN M H. Quality index and hot tearing susceptibility of Al−7Si−0.35Mg−*x*Cu alloys [J]. Transactions of Nonferrous Metals Society of China, 2018, 28: 1275−1286.

[17] SUYITNO, KOOL W H, KATGERMAN L. Hot tearing criteria evaluation for direct-chill casting of an Al−4.5 Pct Cu alloy [J]. Metallurgical and Materials Transactions A, 2005, 36: 1537−1546.

[18] RAPPAZ M, DREZET J M, GREMAUD M. A new hot-tearing criterion [J]. Metallurgical and Materials Transactions A, 1999, 30: 449−455.

[19] KOU S. A criterion for cracking during solidification [J]. Acta Materialia, 2015, 88: 366−374.

[20] HAN J Q, WANG J S, ZHANG M S, NIU K M. Susceptibility of lithium containing aluminum alloys to cracking during solidification [J]. Materialis, 2019, 5: 100203.

[21] ESKIN D G, KATGERMAN. A quest for a new hot tearing criterion [J]. Metallurgical and Materials Transactions A, 2007, 38: 1511−1519.

[22] LI Y, BAI Q L, LIU J C, LI H X, DU Q, ZHANG J S, ZHUANG L Z. The influences of grain size and morphology on the hot tearing susceptibility, contraction, and load behaviors of AA7050 alloy inoculated with Al−5Ti−1B master alloy [J]. Metallurgical and Materials Transactions A, 2016, 47: 4024−4037.

[23] EASTON M A, WANG H, GRANDFIELD J, DAVIDSON C J, STJOHN D H, SWEET L D, COUPER M J. Observation and prediction of the hot tear susceptibility of ternary Al−Si−Mg alloys [J]. Metallurgical and Materials Transactions A, 2012, 43: 3227−3238.

[24] SABAU A S, MIRMIRAN S GLASPIE C, LI S M, APELIAN D, SHYAM A, HAYNES J A, RODRIGUEZ A F. Hot-tearing of multicomponent Al−Cu alloys based on casting load measurements in a constrained permanent mold [C]//146th Annual Meeting & Exhibition Supplemental Proceedings. Pittsburgh: TMS, 2017: 465−473.

[25] WANG Zhi, ZHOU Ye, LI Yi-zhou, WANG Feng, LIU Zheng, MAO Ping-li, JIANG Xiao-ping. Hot tearing behaviors and in-situ thermal analysis of Mg−7Zn−*x*Cu−0.6Zr alloys [J]. Transactions of Nonferrous Metals Society of China, 2018, 28: 1504−1513.

[26] SPITTLE J A, CUSHWAY A A. Influences of superheat and grain structure on hot-tearing susceptibilities of Al−Cu alloy castings [J]. Metals Technology, 1983, 10: 6−13.

[27] GRIFFITH A A. The phenomena of rupture and flow in solids [J]. Philosophical Transactions of the Royal Society of London, 1921, 221: 163−198.

[28] WELLS A A. Application of fracture mechanics and beyond general yielding [J]. British Welding Journal, 1963, 10: 563−570.

[29] EASTON M, WANG H, GRANDFIELD J, STJOHN D, SWEET E. An analysis of the effect of grain refinement on the hot tearing of aluminum alloys [J]. Materials Forum, 2004, 28: 224−229.

[30] SWEET L, EASTON M A, TAYLOR J A, GRANDFIELD G F, DAVIDSON C J, LU L M, COUPER M J, STJOHN D H. Hot tear susceptibility of Al−Mg−Si−Fe alloys with varying iron contents [J]. Metallurgical and Materials Transactions A, 2013, 44: 5396−5407.

[31] FEURER U. Quality Control of engineering alloys and the role of metals science [M]. The Netherlands: Department of Metals Science and Technology of the Delft University of Technology, 1977: 131−145.

[32] CONIGLIO N, CROSS C E. Mechanisms for solidification crack initiation and growth in aluminum welding [J]. Metallurgical and Materials Transactions A, 2009, 40: 2718−2728.

[33] KUBO K, PEHLKE R D. Mathematical modeling of porosity formation in solidification [J]. Metallurgical Transactions B, 1985, 16: 359−366.

[34] KAREH K M, LEE P D, ATWOOD R C, CONNOLLEY T, GOURLAY C M. Revealing the micromechanisms behind semi-solid metal deformation with time-resolved X-ray tomography [J]. Nature Communication, 2014, 5: 4464.

Al−Cu−Mg 合金凝固过程中低熔点共晶体含量与其热裂敏感性之间的关系

韩加强[1]，王俊升[2,3]，张明山[2,3]，牛康民[1]

1. 北京科技大学 材料科学与工程学院，北京 100083；2. 北京理工大学 材料学院，北京 100081；
3. 北京理工大学 前沿交叉科学研究院，北京 100081

摘 要：对三元 Al−Cu−Mg 合金凝固过程中共晶尤其是低熔点共晶含量与热裂敏感性之间的关系进行系统研究。通过控制 Al−Cu−Mg 合金中主合金元素 Cu、Mg 的含量，使合金凝固末期的低熔点共晶体含量不同并对相应的热裂敏感性进行评价。结果表明：凝固末期具有最少量低熔点共晶体的 Al−4.6Cu−0.4Mg(质量分数，%)对热裂最为敏感。在残余液体的总量基本相等的条件下，不同合金成分抗热裂性能与低熔点共晶含量密切相关，合金热裂抗性与低熔点共晶体含量密切相关，即：低熔点共晶含量越高，合金的热裂抗性越好。最后，从凝固过程中的补缩、渗透率以及整体黏度方面讨论低熔点共晶显示出良好热裂抗性的潜在机理。

关键词：Al−Cu−Mg 合金；热裂；凝固；共晶反应；低熔点共晶；热力学

(Edited by Xiang-qun LI)